Nigerian Research Journal of Chemical Sciences **(ISSN: 2682-6054)**
Volume 8, Issue 2, 2020

Analytical Investigations of Irreversible Reactions using a Linear Reactive General Rate Model of Liquid Chromatography

[*1]Abdulaziz G. Ahmad, [2]Abubakar A. Abubakar and [3]Idris M. Idris

[1]Department of Mathematics Programme, National Mathematical Centre, Abuja, Nigeria

[2]Department of Applied Chemistry, Federal University, Dutsen-Ma, Katsina, Nigeria

[3]Department of Chemistry, Nigeria Police Academy, Wudil, Kano-Nigeria

[*]Corresponding Author: agarbaahmad@yahoo.com

ABSTRACT

The present article studied heterogeneous irreversible reaction of type A → B for the linear reactive general rate model (RGRM) of liquid chromatography. The governing model equations comprise an external and intra-particle pore diffusion, axial dispersion, first-order heterogeneous chemical reactions, and interfacial mass transfer. The semi-analytical solutions of the model equations are obtained by the successive application of the Laplace transformation and eigen-decomposition method. The current solutions expand and generalize the recent solutions for single-solute transport in the non-reactive general rate model. For validating the analytical model solutions a scheme of high-resolution finite-volume was applied on the governing model equations to obtain a simulated numerical solution. Scenarios of various studies are analyzed to confirm the accuracy of the semi-analytical solutions and the reliability of the applied numerical technique. The semi-analytical solutions are valuable mechanisms for examining the importance of reactive adsorption affinity, intra-particle pore diffusion and interfacial mass transfer rate on concentration profiles. These results are very useful for chromatography process utilizing diluted (small volume) samples.

Keywords: Chromatographic reactor, Linear adsorption, Linear general rate model, Irreversible reactions

1. INTRODUCTION

High-performance liquid chromatography (HPLC) was developed with aim to further improve the performance of classical column (LC) which allows the flow of a mixture through the column via gravity. HPLC uses a high-pressure pump which allows the mixture to flow into the column along with the solvent and in contrast to the classical LC. This process has potential for

providing efficient separations and more reliable identification of the mixture components. It is applicable in chemical engineering as an effective quantitative chromatographic method for separating mixture components that have distinct adsorption affinities among its components [1]. Various applications of chromatographic methods have been found in the pharmaceutical, chemical, petrochemical, photochemical, food and biotechnological industries. Numerous features which present the HPLC procedures superior to other types of chromatography, are as follows (i) the time for its analysis is short, (ii) it is generally appropriate and hence only a few samples are exempted from the HPLC possibility, (iii) it can be operated on a much larger scale, (iv) HPLC columns can be reused without reconstruction [1-5].

Reactive chromatography is a combined procedure where the chromatographic separation of chemical or biochemical reactions are converted into products and reactants. This methodology increases reactant conversion and product purity and has motivated many scientists in the last few generations [3, 4, 6-16]. In this integrated process, the chemical reactions can be catalyzed homogeneously and heterogeneously. In the case of homogeneous catalysis, account should be taken of the separation of the catalyst. However, in the case of esterification, heterogeneously catalyzed reactions typically occur where the same ion exchange resin serves as a catalyst for the reaction and as an absorbent for separation.

To understand the fundamental concept of a chromatographic reactor with a fixed-bed, a single column reactor and an irreversible reaction of a type $A \rightarrow B$ is considered. The reactant A is dissolved in the desorbent and injected as a rectangular pulse into the column of the stationary phase. The reaction occurs on the catalytic surface to make the product B. Both components A and B interact with the surface of the adsorbent and, due to their diverse affinities to the stationary phase, they migrate inside the column at various velocities of propagation. Therefore, the components are separated and the driving force for the forward reaction is increased while the backward reaction is suppressed. Also, a chemical balance can be performed and a high purity product can be collected from the outlet of the column.

Modeling and simulation of chromatographic processes have become increasingly valuable tools for understanding the underlying transport mechanisms for scaling up physiochemical parameters and for optimizing experimental conditions. There are several models in the literature with different levels of complexity to describe the method [5, 6]. The General Rate Model (GRM) is the most complex and detailed chromatography model among all

the transport models [6]. In GRM, chromatographic separation is controlled by several sorption and transport processes at various levels. The molecules in the sample are transported by convection through the interstitial bulk phase between chromatographic beads but are dispersed due to inhomogeneity of the flow. The analytical solutions of linear chromatographic models can be used to quantify the effect of different mass transfer and reaction kinetics on the process without practical laboratory experiments [4-6, 16-19]. These models are useful for understanding the chromatographic process, as in most situations the volume of the sample injected is small and diluted. The derived analytical solutions could be used to authenticate numerical solutions for more complex models where no experimental data is accessible [5, 6].

In this work, a linear reactive general rate model (RGM) is analyzed to study two-component adsorption equilibria and reaction-separation kinetics in a fixed-bed chromatographic reactor. Semi-analytical solutions of the model are derived for both irreversible and reversible reactions in the particles macrospores. The Laplace transformation and eigen-decomposition technique are successively applied to solve the model equations for Dirichlet boundary conditions (BCs). Due to the complex structure of the solutions, analytical back transformations may not be possible. Therefore, numerical Laplace inversion is applied to get the time domain solutions [6, 12, 20]. To validate the derived solutions, numerical solutions are also obtained by applying a high resolution finite volume scheme to the same model equations [20, 21]. Several case studies are considered and both numerical and semi-analytical results are compared.

This article is structured in the following manner: a brief introduction was presented in Section 1. In Section 2, the linear RGRM is introduced for irreversible reaction along with the Dirichlet BCs. In Section 3, analytical solutions are derived to solve these model equations for an irreversible reaction considered. In Section 4, varieties of test problems are discussed. Finally, in Section 5 Conclusions are drawn.

2. FIXED-BED CHROMATOGRAPHIC REACTOR FOR IRREVERSIBLE REACTION (A →B)

Throughout this system, component A (component 1) is converted to component B (component 2) by irreversible first-order heterogeneous reactions. The reactant and product travel along the column by axial dispersion and conversion of the reactant to the product is due to the first-order chemical reaction in the solid phase. The considered two-component reactive general rate model is based upon the following assumptions: (1) the porous particles in the column are spherical

shaped and have same diameter, (2) the chromatographic process is isothermal , (3) there exist an instantaneous local equilibrium between the macro pore surfaces and the stagnant fluid inside particles macro pores, (4) the concentration gradient in the radial direction are neglected, (5) the diffusional and mass transfer parameters are constant and are independent of the mixing effects of the component involved, (6) interfacial mass transfer between the bulk fluid and particle phases is described by film mass transfer mechanism.

On the basis of the above assumption, the current RGRM contains four mass balance equations for the transport of two-component mixtures, i.e. two equations describe transport in the bulk of the fluid and two equations are for transport within the macro pores of the particles. The one-dimensional mass balance equations of RGRM for the mobile phase of the fluid considered to be a two-component solute percolating through a chromatographic reactor filled with radius spherical particles of R_p are expressed as [5, 6].

$$\frac{\partial c_1}{\partial t} + u\frac{\partial c_1}{\partial z} = D_z\frac{\partial^2 c_1}{\partial z^2} - \frac{3}{R_p}Fk_{ext,i}(c_1 - c_{p,1}|_{r=R_p}), \quad (1)$$

$$\frac{\partial c_2}{\partial t} + u\frac{\partial c_2}{\partial z} = D_z\frac{\partial^2 c_2}{\partial z^2} - \frac{3}{R_p}Fk_{ext,i}\left(c_2 - c_{p,2}|_{r=R_p}\right). \quad (2)$$

In the above equation, z represents the axial coordinate along the column length, t denotes the time coordinate, $c_i(t,z)$ is the concentration of i-th component in the mobile phase of the fluid and $c_{p,i}(t,z)$ is the i-th component concentration in the particles, respectively. Moreover, D_z represents the axial dispersion coefficient, u is the interstitial velocity, $k_{ext,i}$ is the external mass transfer coefficient of i-th component, ε between (0, 1) is the external porosity, $F = \frac{1-\varepsilon}{\varepsilon}$ is the phase ratio and r denotes the radial coordinate of spherical particles of radius R_p.

The corresponding mass balance equations for the solute considering irreversible reactions in the solid phase, along with two mechanisms of intra-particle transport is expressed as [5,6].

$$\varepsilon_p\frac{\partial c_{p,1}}{\partial t} + (1-\varepsilon_p)\frac{\partial q^*{}_{p,1}}{\partial t} = \frac{1}{r^2}\frac{\partial}{\partial r}\left(r^2\left[\varepsilon_p D_{p,1}\frac{\partial c_{p,1}}{\partial r} + (1-\varepsilon_p)D_{s,1}\frac{\partial q^*{}_{p,1}}{\partial r}\right]\right) - (1-\varepsilon_p)\nu_1 q^*_{p,1}, \quad (3)$$

$$\varepsilon_p\frac{\partial c_{p,2}}{\partial t} + (1-\varepsilon_p)\frac{\partial q^*{}_{p,2}}{\partial t} = \frac{1}{r^2}\frac{\partial}{\partial r}\left(r^2\left[\varepsilon_p D_{p,2}\frac{\partial c_{p,2}}{\partial r} + (1-\varepsilon_p)D_{s,2}\frac{\partial q^*{}_{p,2}}{\partial r}\right]\right) + (1-\varepsilon_p)\nu_1 q^*_{p,1}. \quad (4)$$

Here, $q^*{}_{p,i}$ is the local equilibrium concentration of solute in the stationary phase, ε_p is the internal porosity, $D_{p,i}$ is the pore diffusivity of i-th component, $D_{s,i}$ is the surface diffusivity, and ν_i is the reaction rate constant of component 1.

Eqs. (1) - (4) are connected at $r = R_p$ through the subsequent expressions which quantify the temporal change of the average loadings of the particles [6].

$$\left[\varepsilon_p D_{p,1}\frac{\partial c_{p,1}}{\partial r} + (1-\varepsilon_p)D_{s,1}\frac{\partial q^*{}_{p,1}}{\partial r}\right]_{r=R_p} = k_{ext,1}(c_1 - c_{p,1}|_{r=R_p}), \quad (5)$$

$$\left[\varepsilon_p D_{p,2}\frac{\partial c_{p,2}}{\partial r} + (1-\varepsilon_p)D_{s,2}\frac{\partial q^*{}_{p,2}}{\partial r}\right]_{r=R_p} = k_{ext,2}(c_2 - c_{p,2}|_{r=R_p}). \quad (6)$$

In this work, we only considered the linear adsorption isotherms [6].

$$q^*{}_{p,i} = a_1 c_{p,i}, \ i = 1,2. \quad (7)$$

After using Eq. (7) in Eqs. (3) and (4), we obtain

$$a_1^*\frac{\partial c_{p,1}}{\partial t} = \frac{D_{eff}}{r^2}\frac{\partial}{\partial r}\left(r^2\frac{\partial c_{p,1}}{\partial r}\right) - (1-\varepsilon_p)\nu_1 a_1 q_{p,1}^*, \quad (8)$$

$$a_2^*\frac{\partial c_{p,2}}{\partial t} = \frac{D_{eff}}{r^2}\frac{\partial}{\partial r}\left(r^2\frac{\partial c_{p,2}}{\partial r}\right) + (1-\varepsilon_p)\nu_1 a_1 q_{p,1}^*, \quad (9)$$

with,

$$a_i^* = \varepsilon_p + (1-\varepsilon_p)a_i \text{ and } D_{eff,i} = \varepsilon_p D_{p,i} + (1-\varepsilon_p)D_{s,i}a_i, \qquad i = 1,2. \quad (10)$$

Similarly, Eq. (5) and Eq. (6) simplifies to

$$D_{eff,1}\frac{\partial c_{p,1}}{\partial r}|_{r=R_p} = k_{ext,1}(c_1 - c_{p,1}|_{r=R_p}), \quad (11)$$

$$D_{eff,2}\frac{\partial c_{p,2}}{\partial r}|_{r=R_p} = k_{ext,2}(c_2 - c_{p,2}|_{r=R_p}). \quad (12)$$

Furthermore, to facilitate our analysis and reduce the number of variables, the subsequent dimensionless variables are introduced:

$$x = \frac{z}{L}, \ \psi = \frac{ut}{L}, \ \theta = \frac{r}{R_p}, \ P_e = \frac{Lu}{D_z}, \quad \phi_i = \frac{L}{u}\nu_i a_{i,}\zeta = \frac{k_{ext,i}R_p}{D_{eff,i}}, \ \eta_{p,i} = \frac{D_{eff,i}L}{R_p^2 u}, \gamma_{p,i} = 3\zeta_{p,i}\eta_{p,i}F, \quad i = 1,2, \quad (13)$$

where L stand for the column length and $P_e$is representing the Peclet number. By applying the above dimensionless variables in Eqs. (1), (2), (9) and (10), we obtain

$$\frac{\partial c_1}{\partial \psi} + u\frac{\partial c_1}{\partial x} = \frac{1}{P_e}\frac{\partial^2 c_1}{\partial x^2} - \gamma_{p,1}(c_1 - c_{p,1}|_{r=R_p}), \quad (14)$$

$$\frac{\partial c_2}{\partial \psi} + u\frac{\partial c_2}{\partial x} = \frac{1}{P_e}\frac{\partial^2 c_2}{\partial x^2} - \gamma_{p,2}(c_2 - c_{p,2}|_{r=R_p}), \quad (15)$$

$$a_1^*\frac{\partial c_{p,1}}{\partial \psi} = \eta_{p,1}\frac{\partial}{\partial r}\left(\theta^2\frac{\partial c_{p,1}}{\partial r}\right) - (1-\varepsilon_p)\phi_1 c_{p,1}, \quad (16)$$

$$a_2^* \frac{\partial c_{p,2}}{\partial \psi} = \eta_{p,2} \frac{\partial}{\partial r}\left(\theta^2 \frac{\partial c_{p,2}}{\partial r}\right) + \left(1 - \varepsilon_p\right)\phi_2 c_{p,2}. \quad (17)$$

Eqs. (16) and (17) can now be rephrased as

$$a_1^* \frac{\partial}{\partial \psi}\left[\theta c_{p,1}\right] - \eta_{p,1} \frac{\partial^2}{\partial \theta^2}\left[\theta c_{p,1}\right] + \left(1 - \varepsilon_p\right)\phi_1\left[\theta c_{p,1}\right] = 0, \quad (18)$$

$$a_2^* \frac{\partial}{\partial \psi}\left[\theta c_{p,2}\right] - \eta_{p,2} \frac{\partial^2}{\partial \theta^2}\left[\theta c_{p,2}\right] + \left(1 - \varepsilon_p\right)\phi_2\left[\theta c_{p,2}\right] = 0, \quad (19)$$

Moreover, the suitable inlet and outlet BCs are required for Eqs. (14), (15), (18) and (19). For an initially regenerated column, the corresponding initial conditions of Eqs. (14) and (15)} are stated as

$$c_i(0, x) = 0, \qquad (0 < x < 1) \qquad i = 1,2 \quad (20)$$

and initial conditions for Eqs. (18) and (19), considering empty particles, are expressed as

$$q_{p,i}^*(0, x, \theta) = 0, \quad c_{p,i}(0, x, \theta) = 0, \quad x, r \in (0,1). \quad (21)$$

Because of the assumed desorption rates or rapid adsorption, the concentrations of solute in the pores and that in the stationary phase are in equilibrium state. Moreover, The Dirichlet BCs considered for Eqs. (14) and (15), in this current study is expresses as

2.1 Inlet Dirichlet BCs

The simpler Dirichlet BCs are utilized at the column inlet in this case:

$$c_i(\psi, x = 0) = \begin{cases} c_{inj,i,} & if\ 0 \le \psi \le \psi_{inj,} \\ 0, & \psi > \psi_{inj,} \end{cases} \quad (22a)$$

together with zero Neumann BCs for a hypothetically infinite length column:

$$\frac{\partial c_i}{\partial x}\Big|_{x=\infty} = 0, \quad (22b)$$

In the above equation, ψ_{inj} stand for the time of sample injection. For sufficiently small dispersion coefficient, for example $D_z \le 10^{-5} m^2/s$ the Dirichlet inlet boundary conditions are well applicable.

3. RGRM ANALYTICAL SOLUTIONS FOR REACTION OF TYPE A → B

In this section, semi-analytical solutions of linear RGRM (c.f. Eqs. (14), (15), (18) and (19)) are derived for Dirichlet (Eqs. (22a) and (22b)). The model can be conveniently solved by means of a Laplace transformation defined as

$$\bar{c}(s,x) = \int_0^\infty e^{-s\psi} c(\psi,x) d\psi, \psi \geq 0. \tag{23}$$

The Laplace transformations of model Eqs. (14) and (15) generate

$$s\bar{c}_1 + \frac{\partial \bar{c}_1}{\partial x} = \frac{1}{P_e}\frac{\partial^2 \bar{c}_1}{\partial x^2} - \gamma_{p,1}(\bar{c}_1 - \bar{c}_{p,1}|_{p=1}), \tag{24}$$

$$s\bar{c}_2 + \frac{\partial \bar{c}_2}{\partial x} = \frac{1}{P_e}\frac{\partial^2 \bar{c}_2}{\partial x^2} - \gamma_{p,2}\left(\bar{c}_2 - \bar{c}_{p,2}|_{p=1}\right). \tag{25}$$

While, the Laplace transformations of Eqs. (18) and (19) give

$$\eta_{p,1}\frac{d^2}{d\theta^2}\left[\theta\bar{c}_{p,1}\right] - \frac{a_1^*}{\eta_{p,1}}\left[\theta\bar{c}_{p,1}\right] - \frac{(1-\varepsilon_p)\phi_1}{\eta_{p,1}}\left[\theta\bar{c}_{p,1}\right] = 0, \tag{26}$$

$$\eta_{p,2}\frac{d^2}{d\theta^2}\left[\theta\bar{c}_{p,2}\right] - \frac{a_2^*}{\eta_{p,2}}\left[\theta\bar{c}_{p,2}\right] - \frac{(1-\varepsilon_p)\phi_2}{\eta_{p,2}}\left[\theta\bar{c}_{p,2}\right] = 0. \tag{27}$$

The general solution of Eq. (26) is given as

$$\bar{c}_{p,1}(s,x,\theta) = \frac{1}{\theta}\left[k_1 e^{\sqrt{\alpha(s)}\theta} + k_2 e^{-\sqrt{\alpha(s)}\theta}\right], \tag{28}$$

where,

$$\alpha(s) = \frac{a_1^* s + (1-\varepsilon_p)\phi_1}{\eta_{p,1}}. \tag{29}$$

By applying the boundary conditions given in Eq. (22a), the values of k_1 and k_2 in Eq. (28) is obtain as

$$k_{1,2} = \pm \frac{\zeta_{p,1}\bar{c}_1}{2(\sinh\sqrt{\alpha(s)})\left[\sqrt{\alpha(s)}\coth\left(\sqrt{\alpha(s)}\right) + \zeta_{p,1} - 1\right]}. \tag{30}$$

Here, the upper positive sign is taken for k_1 and the lower negative sign for k_2. At $\theta = 1$, Eqs. (28) and (30) reduce to

$$\bar{c}_{p,1}|_{\theta=1} = \bar{c}_1 f_1(s), \tag{31}$$

where,

$$f_1(s) = \frac{\zeta_{p,1}}{\left[\sqrt{\alpha(s)}\coth\left(\sqrt{\alpha(s)}\right) + \zeta_{p,1} - 1\right]}. \tag{32}$$

After introducing Eq. (31) in Eq. (27), we obtain the general solution as

$$\bar{c}_{p,2}(s,x,\theta) = \frac{1}{\theta}\left[k_1' e^{\sqrt{\alpha(s)}\theta} + k_2' e^{-\sqrt{\alpha(s)}\theta}\right] + \frac{f_1(s)(1-\varepsilon_p)\phi_1 \bar{c}_1}{a_2^*}. \quad (33)$$

Where $\alpha'(s) = \frac{a_2^*}{\eta_{p,2}}$, by applying Eq. (22a) in (33), we obtain

$$k_{1,2}' = \pm \frac{\zeta_{p,2}\bar{c}_2 - \frac{\zeta_{p,2} f_1(s)(1-\varepsilon_p)\phi_1 \bar{c}_1}{a_2^*}}{2(\sinh\sqrt{\alpha'(s)})\left[\sqrt{\alpha'(s)}\coth\left(\sqrt{\alpha'(s)}\right) + \zeta_{p,2} - 1\right]}, \quad (34)$$

At $\theta = 1$, Eqs. (33) and (34) reduce to

$$\bar{c}_{p,2}|_{\theta=1} = \bar{c}_2 f_2(s) + \bar{c}_1 \Psi(s), \quad (35)$$

where,

$$f_2(s) = \frac{\zeta_{p,2}}{\left[\sqrt{\alpha'(s)}\coth\left(\sqrt{\alpha'(s)}\right) + \zeta_{p,2} - 1\right]}. \quad (36)$$

and

$$\Psi(s) = \frac{f_1(s)(1-\varepsilon_p)\phi_1}{a_2^*}\left[\frac{-\zeta_{p,2}}{\left[\sqrt{\alpha'(s)}\coth\left(\sqrt{\alpha'(s)}\right) + \zeta_{p,2} - 1\right]} + 1\right]. \quad (37)$$

After introducing Eqs. (31) and (35) in Eqs. (24) and (25), respectively, we get the following ordinary differential equations (ODEs)

$$\frac{d^2\bar{c}_1}{dx^2} - P_e\frac{d\bar{c}_1}{dx} - P_e\beta_1(s)\bar{c}_1 = 0, \quad (38)$$

$$\frac{d^2\bar{c}_2}{dx^2} - P_e\frac{d\bar{c}_2}{dx} - P_e\beta_2(\mathrm{s})\Psi(s)\bar{c}_1 = 0, \quad (39)$$

where

$$\beta_1(s) = s + \gamma_{p,1}\left(1 - f_1(s)\right), \qquad \beta_2(s) = s + \gamma_{p,2}\left(1 - f_2(s)\right). \quad (40)$$

In the matrix notions, Eqs. (38) and (39) can be expressed as

$$\frac{d^2}{dx^2}\begin{pmatrix}\bar{c}_1\\ \bar{c}_2\end{pmatrix} - P_e\frac{d}{dx}\begin{pmatrix}\bar{c}_1\\ \bar{c}_2\end{pmatrix} - \begin{bmatrix}P_e\beta_1(s) & 0\\ -P_e\beta_2(\mathrm{s})\Psi(s) & P_e\beta_2(s)\end{bmatrix}\begin{pmatrix}\bar{c}_1\\ \bar{c}_2\end{pmatrix} = \begin{pmatrix}0\\ 0\end{pmatrix}. \quad (41)$$

Here, the curly brackets ( ) represents a column vector, the square brackets [ ] stands for a square matrix, and $\bar{c}_i$ for $i = 1,2$ are the liquid phase concentrations of mixture components in the Laplace domain.

The reaction coefficient matrix $[\beta]$ on in Eq. (41) is given as

$$\beta = \begin{bmatrix} P_e\beta_1(s) & 0 \\ -P_e\beta_2(s)\Psi(s) & P_e\beta_2(s) \end{bmatrix}. \tag{42}$$

In the next step, linear transformation matrix [A] will be computed [22]. Note that, the columns of [A] are the eigenvectors of the matrix $[\beta]$. The eigenvalues and

Eigen vectors of the matrix $[\beta]$ are given as:

$$\lambda_1 = P_e\beta_1(s), \quad x_1 = \begin{pmatrix} A_{11} \\ \frac{-\gamma_{p,2}P_e\Psi(s)A_{11}}{P_e\beta_1(s)-P_e\beta_2(s)} \end{pmatrix}, \quad and \ \lambda_2 = P_e\beta_2(s), \quad x_2 = \begin{pmatrix} 0 \\ A_{11} \end{pmatrix}. \tag{43}$$

Here, λ_1 and λ_2 denote the eigenvalues and A_{11} and A_{22} are the arbitrary constants. For simplicity, we take the values of A_{11} and A_{22} equal to one. Using Eq. (43), the diagonal matrix κ and the transformation matrix [A] can be written as

$$\kappa = \begin{bmatrix} P_e\beta_1(s) & 0 \\ 0 & P_e\beta_2(s) \end{bmatrix}, \qquad A = \begin{bmatrix} 1 & 0 \\ \frac{-\gamma_{p,2}P_e\Psi(s)}{P_e\beta_1(s)-P_e\beta_2(s)} & 1 \end{bmatrix}. \tag{44}$$

The matrix [A] is then used in the following linear transformation [22].

$$\begin{pmatrix} \bar{c}_1 \\ \bar{c}_2 \end{pmatrix} = \begin{bmatrix} 1 & 0 \\ \frac{-\gamma_{p,2}P_e\Psi(s)}{P_e\beta_1(s)-P_e\beta_2(s)} & 1 \end{bmatrix} \begin{pmatrix} b_1 \\ b_2 \end{pmatrix}. \tag{45}$$

Applying the above linear transformation on Eq. (41), we get

$$\frac{d^2}{dx^2}\begin{pmatrix} b_1 \\ b_2 \end{pmatrix} - P_e\frac{d}{dx}\begin{pmatrix} b_1 \\ b_2 \end{pmatrix} = \begin{bmatrix} P_e\beta_1(s) & 0 \\ 0 & P_e\beta_2(s) \end{bmatrix}\begin{pmatrix} b_1 \\ b_2 \end{pmatrix}. \tag{46}$$

Eq. (46) represents a system of two independent ODEs. Their explicit solutions are given as

$$b_1(s,x) = A_1e^{m_1x} + B_1e^{-m_2x}, \qquad m_{1,2} = \frac{P_e}{2}\left(1 \pm \sqrt{1 + \frac{4\beta_1(s)}{P_e}}\right), \tag{47}$$

and

$$b_2(s,x) = A_2e^{m_3x} + B_2e^{-m_4x}, \qquad m_{3,4} = \frac{P_e}{2}\left(1 \pm \sqrt{1 + \frac{4\beta_2(s)}{P_e}}\right), \tag{48}$$

Here, A_1, A_2, B_1 and B_2 are constants of integration which can be obtained by using the selected BCs.

3.1 Dirichlet BCs

The Laplace Transformation of Eqs. (22a) and (22b) are given as

$$\bar{c}_i(s,0) = \frac{c_{inj,i}(1-e^{-s\psi_{inj}})}{s}, \qquad \frac{d\bar{c}_i}{dx}(s,\infty) = 0. \tag{49}$$

On using the transformations in Eq. (45), Eq. (49) yields

$$\bar{b}_1(s,x=0) = \frac{c_{inj,1}(1-e^{-s\psi_{inj}})}{s}, \qquad \frac{d\bar{b}_1}{dx}(s,\infty) = 0. \tag{50}$$

$$\bar{b}_2(s,x=0) = \frac{c_{inj,2}(1-e^{-s\psi_{inj}})}{s} + \frac{\gamma_{p,2}P_e\Psi(s)}{P_e\beta_1(s)-P_e\beta_2(s)}\bar{b}_1(s,x=0), \qquad \frac{d\bar{b}_2}{dx}(s,\infty) = 0. \tag{51}$$

After applying these boundary conditions on Eq. (47), the values of A_1 and B_1 are obtained as

$$A_{1=}\frac{c_{inj,1}(1-e^{-s\psi_{inj}})}{s}, \qquad B_1 = 0. \tag{52}$$

Thus, Eqs. (45), Eq. (57) and Eq. (52) give

$$\bar{c}_1(s,x) = \frac{c_{inj,i}(1-e^{-s\psi_{inj}})}{s}e^{m_1 x}. \tag{53}$$

The value of m_1 is given by Eq. (47) for the upper negative sign. Similarly, on using Eq. (51) in Eq. (48), we get the values of A_2 and B_2 as follows:

$$A_2 = \frac{(1-e^{-s\psi_{inj}})}{s}\left[c_{inj,2} + \frac{\gamma_{p,2}P_e\Psi(s)}{P_e\beta_1(s)-P_e\beta_2(s)}c_{inj,1}\right], \qquad B_2 = 0. \tag{54}$$

With these values of $A_2$and B_2 and using Eq. (45) in Eq. (48), we obtain

$$\bar{c}_2(s,x) = \frac{c_{inj,1}(1-e^{-s\psi_{inj}})}{s}\left(\frac{\gamma_{p,2}\Psi(s)}{\beta_1(s)-\beta_2(s)}\right)(e^{m_3 x}-e^{m_1 x}) + \frac{c_{inj,2}(1-e^{-s\psi_{inj}})}{s}e^{m_3 x}. \tag{55}$$

Analytical Laplace inversions are not possible to bring back solutions in the time domain ψ. Therefore, the numerical inverse Laplace transformation is employed to find the original solutions $c_j(\psi,x)$ for j=1,2. In this work, an efficient numerical Laplace inversion method, based on a Fourier series expansion is applied as explained below [21, 24].

The solution in the time domain $c_j(\psi,x)$ can be obtained by using the exact formula for the back transformation as

$$c_j(\psi,x) = L^{-1}\left[\bar{c}_j(s,x)\right] = \frac{1}{2\pi i}\int_{v-i\infty}^{v+i\infty} e^{-ts}\bar{c}_j(s,x)ds, \quad j = 1,2. \tag{56}$$

With $s = v + iw;\ \ v,w \in \mathbb{R}$. The real constant v exceeds the real part of all the singularities of $\bar{c}_j(s,x)$. The integrals in Eqs. (23) and (56) exist for $\mathrm{Re}(s) > \tilde{\alpha} \in \mathbb{R}$ if

(a) c_j is locally integrable,

(b) There is a $\psi_0 \geq 0$ and $p, \tilde{\alpha} \in \mathbb{R}$, such that $c_j(\psi,x) \leq pe^{\tilde{\alpha}\psi}$ for all $\psi \geq \psi_0$,

(c) for all $\psi \in (0,\infty)$ there is a neighborhood in which c_j is of bounded variation.

In the following we always assume that c_j fulfils the above conditions and in addition that there are no singularities of $\bar{c}_j(s,x)$ to the right of the origin. Therefore, Eqs. (23) and 56) are defined for all $y > 0$. The possibility to choose $v > 0$arbitrarily, is the basis of the methods of Durbin [23]. The integral in Eq. (56) is equivalently expressed in the interval [0, 2T] as

$$c_j(\psi,x) = \frac{e^{v\psi}}{\pi}\int_0^{\infty}\left[R_e\{\bar{c}_j(s,x)\}\cos(w\psi) - I_m\{\bar{c}_j(s,x)\}\sin(w\psi)\right]dw. \tag{57}$$

Durbin derived the following approximate expression for Eq. (57):

$$c_j(\psi,x) = \frac{e^{v\psi}}{T}\left[-\frac{1}{2}R_e\{\bar{c}_j(v,x)\} + \sum_{p=0}^{\infty} R_e\left\{\bar{c}_j\left(v + i\frac{p\pi}{T},x\right)\right\}\cos\left(\frac{p\pi\psi}{T}\right) - \sum_{p=0}^{\infty} I_m\left\{\bar{c}_j\left(v + i\frac{p\pi}{T},x\right)\right\}\sin\left(\frac{p\pi\psi}{T}\right)\right]. \tag{58}$$

In the numerical computations, the infinite series in Eq. (58) can only be summed up to a finite number N_p of terms only. Thus, a truncation error occurs in the numerical computations. In this work, the numerical Laplace inversion formula in Eq. (58) is applied to obtain the time domain solution $c_j(\psi,x)$ by considering $N_p = 10^3$.

4. NUMERICAL TEST PROBLEMS

By considering multiple test problems, the derived semi-analytical solutions described in the previous sections were examined. For verification, the numerical solutions are compared with the derived semi-analytical solutions of two-component of the same model. These numerical solutions are obtained by implementing a high resolution finite volume scheme (HR-FVS) of Koren [22]. A general collection of essential model parameters employed in the test problems is provided in Table 1. In order to obtain consistent results, the values for these parameters were taken in typical ranges. The assumption has been made for $D_{eff,i}$ and $k_{ext,i}$ tobe equal for all components.

4.1 Linear irreversible reaction

In this section, the semi-analytical and numerical solutions of the model equations Eqs. (1)- (4) are compared for the considered irreversible reaction in the solid phase. The results obtained illustrate the effects of reaction rate constant ω_1, boundary conditions, Peclet number P_e, intra-particle diffusion resistance η and film mass transfer resistance ζ_P on the concentration profiles.

Figure 1 displays the effects of injected sample volume on the concentration profiles. Concentration profiles are plotted at the column outlet when a rectangular pulse of finite width, is injected into an empty column using Dirichlet BCs ($c_{\mathrm{in}j,\mathrm{i}} = 0.5g/l$ for $i = 1,2$). In Figure 1(a), the same amount of injections shall be taken for both components (i.e.$c_{\mathrm{in}j,1} = 0.5g/l$, $c_{\mathrm{in}j,2} = 0.5g/l$) together with the constant reaction rate $\omega_1 = 0.1$. The quantity of the product (component 2) increases as a result of the conversion of the reactant (component 1) to the product by the irreversible reaction. Contrarily, in Figure 1(b), the amount of product (component 2) is$c_{\mathrm{in}j,1} = 0.25g/l$, while the injection amount for reactant (component 1) is $c_{\mathrm{in}j,1} = 0.5g/l$,. Here, the same quantity of reactant (component 1) is transformed into the product (component 2), so the total quantity of the drug is equal to the quantity of converted reactant plus the quantity of injected product. Because of the smaller amount of the product injected, the height of component 2 in Figure 1(b) is less than that in Figure 1(a). Moreover, it can be seen that component 1 elutes later than component 2 because of a variety in their affinities (i.e $a_1 = 2.5$ and $a_2 = 0.5$). In all the cases, the numerical solutions and semi-analytical are in great satisfaction with one another.

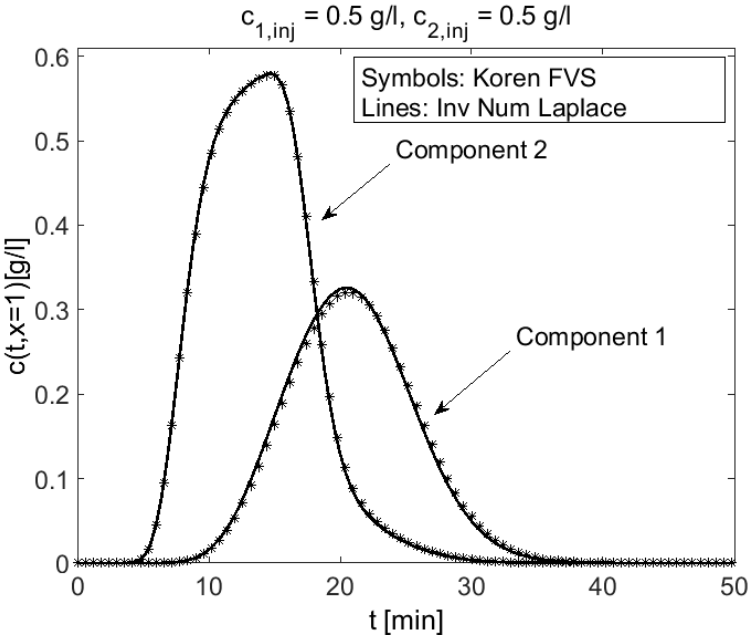

Figure 1(a): Irreversible reaction: Effects of injection on the concentration profiles obtained by Dirichlet BCs at $x = 1$. Here, $\omega_1 = 0.1$ & $\omega_2 = 0.05$. Other remaining parameters are given in Table 1

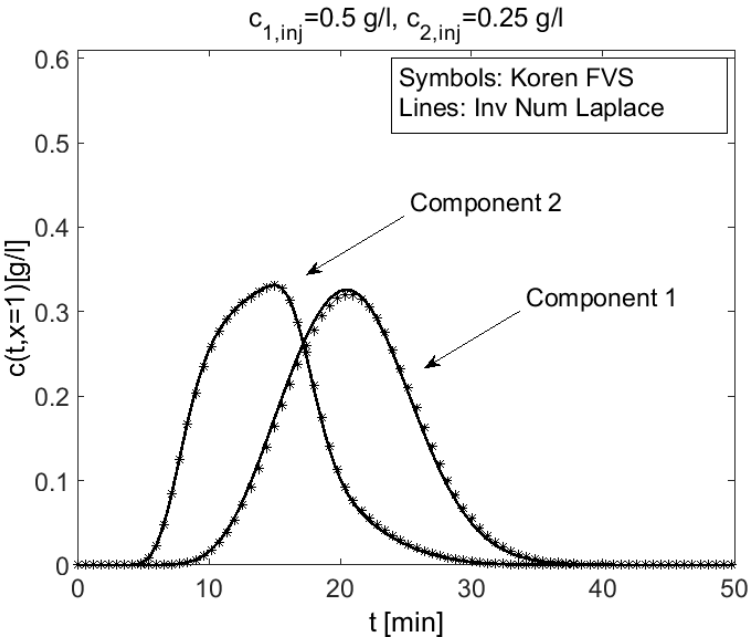

Figure 1(b): Irreversible reaction: Effects of injection on the concentration profiles obtained by Dirichlet BCs at $x = 1$. Here, $\omega_1 = 0.2$ & $\omega_2 = 0.02$. Other remaining parameters are given in Table 1

Figure 2 illustrates the consequences of reaction rate constant $\omega_{\mathrm{i}},\ i = 1,2$ on the concentration profiles. The concentration profiles are plotted by employing Dirichlet BCs and taking ω_1 as a parameter. Here, $c_{\mathrm{in}j,1} = 0.5g/l,\ c_{\mathrm{in}j,2} = 0.5g/l$ and $c_{\mathrm{i},init} = 0.0g/l$ were used. For this case, the quantity of product improves on raising the value of reaction rate constant, while the quantity of reactant is reducing.

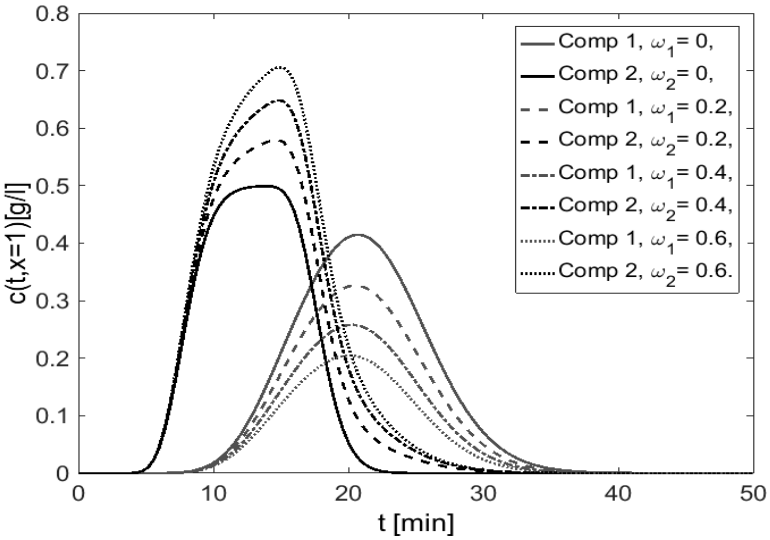

Figure 2: Irreversible reaction: Effects of reaction rate constant $\omega_{\mathrm{i}},\ i = 1,2$ on the concentration profiles at $x = 1$, using Dirichlet BCs. Here, $c_{\mathrm{in}j,1} = 0.5\ g/l$,$c_{\mathrm{in}j,2} = 0.5\ g/l$. The remaining parameters are given in Table 1.

Figure 3(a) shows the influences of Biot number,$\zeta_P = \frac{k_{ext}R_p}{D_{eff,i}}$, on the concentration profiles of both components for different three values of ζ_P.For $\zeta_P = 50$, for $\zeta_P = 05$, both components have steeped profiles whereas the peak profiles are broadened. Figure 3(b) investigates the impacts of intra-particle diffusionη on the concentration profiles. The concentration profiles for both components are plotted for a fixed $P_e = 125$ and practising some distinct values of η. For $\eta = 0.02$, there is a reduction of column retention time for both components because of the slow diffusion rate, whereas, for $\eta = 20$ the retention time for both components improves. In addition, the rising value of $\eta = 0.02$improves the separation of both components. Insufficiencies in intra-particle mass transfer resistances of both components decrease the spreading time for the considered fully porous adsorbents.

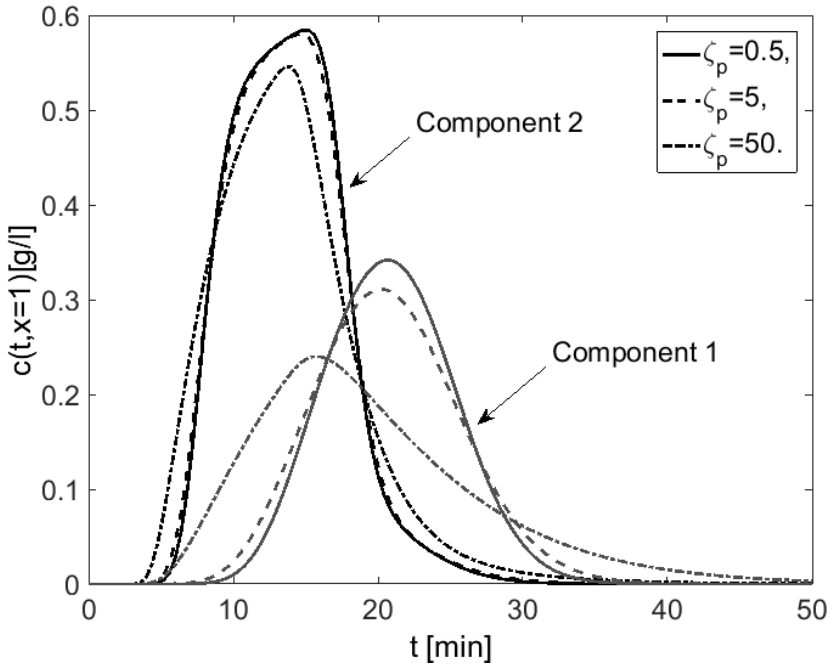

Figure 3(a): Irreversible reaction: Influences of ζ_P on the concentration profiles. Other remaining parameters are given in Table 1

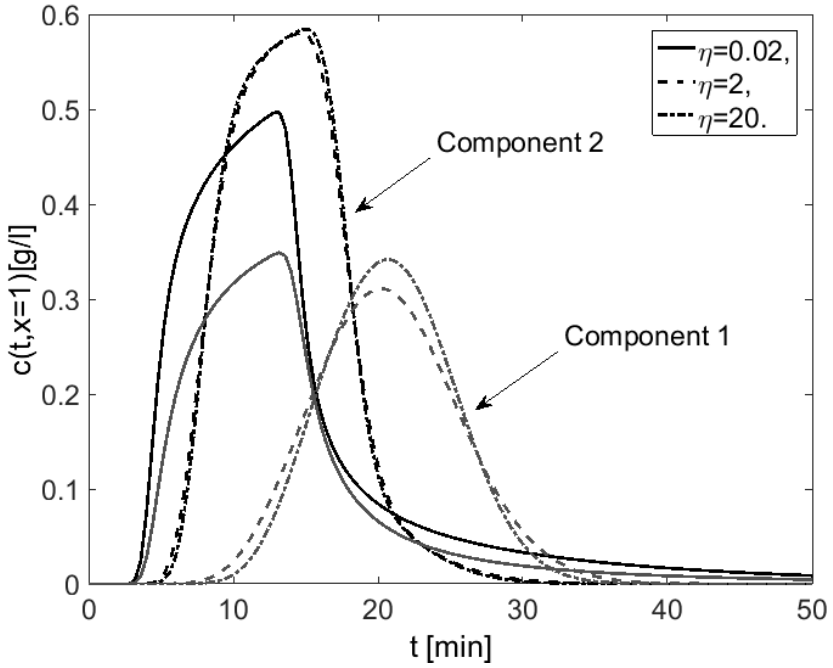

Figure 3(b): Irreversible reaction: Influences of η on the concentration profiles. Other remaining parameters are given in Table 1

5. CONCLUSION

A two-component irreversible reaction for linear reactive general rate model was developed and solved using Dirichlet boundary condition to obtain the semi-analytical solutions. Also, the complete analytical solutions in the Laplace domain were obtained, by use of the Laplace transformation technique. The numerical Laplace inversion was employed to obtain the desired actual-time domain for the concentration profiles. The accuracy for the numerical results of a second-order finite volume scheme against semi-analytical results was conducted. Clear agreements between numerical and semi-analytical tests confirmed the accuracy of the analytical expressions and the correctness of the proposed numerical method. The derived semi-analytical solutions are useful tools to investigate the impact of reaction rate constants, interfacial mass transfer rate, adsorption affinity, and intra-particle pore diffusion on the concentration profiles. This analytical procedure can also be applied to the confirmation of the result obtained by the use of a numerical scheme carried out in this current article.

Table 1: Referenece parameters used in the numerical test problems.

Parameters	Values
Interstitial velocity	$u = 2.5\ cm/min$
Column length	$L = 10\ cm$
Effective dispersion coefficient	$D_z = 0.34\ cm^2/min$
External mass transfer coefficient	$D_{eff} = 10^{-4} cm^2/min$
Axial dispersion coefficient	$k_{ext} = 0.01\ cm/min$
External porosity	$\epsilon = 0.4$
Internal porosity	$\epsilon_p = 0.333$
Initial concentrations	$c_{inj,1} = 0\ g/l$
Concentration at inlet for component 1	$c_{inj,2} = 0\ g/l$
Concentration at inlet for component 2	$a_1 = 2.5$
Adsorption equilibrium constant for component 1	$a_2 = 0.5$
Adsorption equilibrium constant for component 2	$\omega_1 = 0.1$
Reaction rate constant (component 1)	$\omega_2 = 0.05$
Reaction rate constant (component 2)	$t_{max} = 40$
Total simulation time	

REFERENCES

1. Meyer, V. R. (2013). Practical high-performance liquid chromatography. *John Wiley & Sons.*
2. Ruthven, D.M. (1984). Principles of adsorption and adsorption processes. *Wiley-Interscience, New York.*
3. Ganetsos, G. & Barker, P.E. (1993). Preparative and production scale chromatography (vol. 61). *Marcel Dekker, Inc.*, New York, 375-523.
4. Li, P., Xiu, G. & Rodrigues, A.E. (2003). Analytical solutions for breakthrough curves in a fixed bed of shell-core adsorbent, *AIChE J.*, 49, 2974-2979
5. Guiochon, G., Felinger, A., Shirazi, D.G. & Katti, A.M. (2006). Fundamentals of preparative and nonlinear chromatography, 2nd ed. *Elsevier Academic Press, New York.*
6. Schweich, D. & Villermaux, J., (1978). The chromatographic reactor. A new theoretical approach. *Ind. Eng. Chem. Fundamen,* 17, 1-7.
7. Cho, B.K., Aris, R. & Carr, R.W., (1982). The mathematical theory of a countercurrent catalytic reactor. *Proc. R. Sot. Lond*. 383, 147-189.
8. Takeuchi, K. & Uraguchi, Y. (1976). Separation conditions of the reactant and the product with a chromatographic moving bed reactor. *J. Chem. Eng. Japan, 9*, 164-166.
9. Takeuchi, K. & Uraguchi, Y. (1977). Experimental studies of a chromatographic moving-bed reactor-catalytic oxidation of carbon monoxide on activated alumina as a model reactor, *J. Chem. Eng. Japan, 10,* 455-460
10. Takeuchi, K., Miyauchi, T. & Uraguchi, Y. (1978). Computational studies of a chromatographic moving bed reactor for consecutive and reversible reactions. *J. Chem. Eng. Japan*, *11*, 216-220.
11. Binous, H. & McCoy, B. (1992). Chromatographic reactions of the three components: Application to separations. *Chem. Eng. Sci*., 47, 4333-4343
12. Borren, T., Fricke, J. & Schmidt-Traub, H. (Eds.), (2005). Chromatographic Reactors in Preparative Chromatography of Fine Chemicals and Pharmaceutical Agents. *Wiley-VCH Verlag, Weinheim*, 371-395.
13. Parris, N. A. (2000). Instrumental liquid chromatography: a practical manual on high-performance liquid chromatographic methods. *Elsevier.*

14. Yamaoka, K. & Nakagawa, T. (1976). Moment analysis for reaction chromatography. *J. Chromatogr. A.* 117, 1-10.
15. Sardin, M., Schweich, D., Villermaux, J., Ganetsos, G. & Barker, P.E. (Eds.), (1993). Preparative fixed-bed chromatographic reactor, preparative and production scale chromatography. *Marcel Dekker Inc., New York, USA*, 477.
16. Rodrigues, A. & Tondeur, D. (1975). Influence of axial dispersion on chemical conversion. Application to reactor design, *Rev. Port. Quim*. 17, 183-190.
17. Rosen, J. B., (1952). Kinetics of a fixed bed system for solid diffusion into spherical particles. *J. Chem. Phys.* 20(3), 387-394.
18. Massaldi. H. A. & Gottifredi, J. C. (1972). Adsorption dansun lit fixe-cas de trois resistances simultaneous. *Chem. Eng. Sci*., 27, 1951-1956.
19. Lin, B., Song, F. & Guiochon, G. (2003). Analytical solution of the ideal, nonlinear model of reaction chromatography for a reaction A→ B and a parabolic isotherm. *J. Chromatogr. A.* 1003, 91-100.
20. Dolan, J. W., Gant, J. R., & Snyder, L. R. (1979). Gradient elution in high-performance liquid chromatography: II. Practical application to reversed-phase systems. *Journal of Chromatography A, 165*(1), 31-58.
21. Ahmad, A. G. (2015). Comparative Study of Bisection and Newton-Rhapson Methods of Root-Finding Problems. *Int. J. of Mathematics Trends and Tech*, 19(2).
22. Koren, B., (1993). A robust upwind discretization method for advection, diffusion and source terms. Numerical Methods for Advection-Diffusion Problems, *Vieweg Verlag, Braunschweig*, Volume 45 of Notes on Numerical Fluid Mechanics, chapter 5, pages 117-138,
23. Quezada, C.R., Clement, T.P. & Lee, K.K. (2004). Generalized solution to multi-dimensional multi-species transport equations coupled with a first-order reaction network involving distinct retardation factors. *Advances in water resources*. 27, 507-520.
24. Durbin, F. (1974). Numerical Inversion of Laplace Transforms: An efficient improvement to Dubner and Abate's Method. *The Computer J*. 17, 371-376.